



James, O. N., Hilton, G., & Beach, M. (2017). Radiation Efficiency Analysis of Balanced-Impedance Hexaferrite Substrate for Antenna Miniaturisation. In *2017 Loughborough Antennas & Propagation Conference (LAPC 2017)* (pp. 11-15). Institution of Engineering and Technology (IET). <https://doi.org/10.1049/cp.2017.0235>

Peer reviewed version

License (if available):  
Unspecified

Link to published version (if available):  
[10.1049/cp.2017.0235](https://doi.org/10.1049/cp.2017.0235)

[Link to publication record in Explore Bristol Research](#)  
PDF-document

This is the author accepted manuscript (AAM). The final published version (version of record) is available online via IET at <http://digital-library.theiet.org/content/conferences/10.1049/cp.2017.0235> . Please refer to any applicable terms of use of the publisher.

## University of Bristol - Explore Bristol Research

### General rights

This document is made available in accordance with publisher policies. Please cite only the published version using the reference above. Full terms of use are available:  
<http://www.bristol.ac.uk/red/research-policy/pure/user-guides/ebr-terms/>

# Radiation Efficiency Analysis of Balanced-Impedance Hexaferrite Substrate for Antenna Miniaturisation

*O N James, G S Hilton, M A Beach*

*Communications Systems and Networks Group, University of Bristol, oliver.james@bristol.ac.uk*

**Keywords:** Antenna miniaturisation, electrically small antennas, hexagonal ferrite, radiation efficiency, radiation patterns.

## Abstract

Antenna miniaturisation in the low UHF band is required since the wavelengths are large compared to portable consumer terminals. Magneto-dielectric substrates such as hexaferrites which increase  $\mu_r$  as well as  $\epsilon_r$  have received attention for their miniaturisation potential, however there is a shortage of published results for the radiation efficiency of such antennas based on full 3D radiative characterisation in free space conditions. In this work, patch antennas fabricated on hexaferrite, FR-4 and RT5880 substrates were examined through simulation, fabrication and radiative measurement. While the frequency in hexaferrite was reduced by a factor of six compared to the RT5880 antennas, the efficiency in the hexaferrite antennas was low. The combined effect of the losses in the hexaferrite and the electrically small size of the resulting patch antenna limits its use in long range transmitting applications, though it may still find application in short range or receiver applications.

## 1 Introduction

There is an ongoing need for antenna developments in the low UHF band below 1000 MHz. Vacation of the analogue TV broadcast bands offers the opportunity to deploy “whitespace” devices in the band 470–790 MHz [1, 2]. Similarly, control-plane communications for 5G and increasing volume of machine-to-machine communication can utilise the long-range, low-data rate channels associated with the low UHF band. Alternatively, short range UHF applications exist in the context of RFID readers and wireless medical devices [3]. In any of these cases the wavelengths involved necessitate antenna miniaturisation in consumer devices.

Many examples exist of patch antenna miniaturisation with a substrate of dielectric permittivity  $\epsilon_r$ . While the patch antenna offers favourable broadbeam radiation pattern characteristics and reasonable efficiency provided the dielectric losses are low [4], the miniaturisation offered by the wavelength compression potentially requires very high dielectric permittivity values  $\epsilon_r$  to compress the large wavelengths into an acceptable volume. The patch antenna is known to be intrinsically relatively narrowband

compared to the half-wavelength wire dipole for example [4], with the bandwidth still further reduced by increased  $\epsilon_r$  [5].

Magneto-dielectric substrate materials have been proposed to counter the bandwidth problems associated with patch antenna miniaturisation [5]. Increasing both magnetic permeability  $\mu_r$  and  $\epsilon_r$  greatly increases the resultant antenna miniaturisation, reducing the bandwidth reduction associated with high values of increasing  $\epsilon_r$  [5]. While magneto-dielectric loading elements have been tested in various forms to provide varying degrees of antenna miniaturisation [3, 6, 7, 8, 9, 10, 11, 12], there is a shortage of works recording the full 3D radiative characterisation of these antennas using these substrates.

In this work a balanced-impedance hexaferrite (HXF) material, as well as samples of FR-4 and Rogers RT5880, were characterised using a Keysight E4991B impedance analyser. The 3D radiation patterns and efficiency characteristics of patch antennas built on these substrates were then analysed in simulation (CST Microwave Studio) and free space radiative measurement.

## 2 Background

### 2.1 Balanced wave impedance and hexaferrites

A theoretical lossless magneto-dielectric substrate for patch antennas was examined in [5]. That work inspired many others by noting that patch antenna bandwidth would be degraded more slowly with increasing miniaturisation factor  $n = \sqrt{\mu_r \times \epsilon_r}$ , if increased  $\mu_r$  was used to provide some of the increase in refractive index  $n$  as opposed to increasing  $\epsilon_r$  in isolation. In addition to achieving high  $n$ , various authors have attempted to satisfy the “balanced wave impedance” criterion during material design [7, 13], wherein satisfying  $\mu_r = \epsilon_r$  causes the material to exhibit the same wave impedance as free space [13], giving the patch similar bandwidth to the same-sized patch with no substrate [5]. The wave impedance  $Z$  is given by:

$$Z = \sqrt{\frac{\mu_r}{\epsilon_r}} \times 377 \, \Omega \quad (1)$$

For antenna applications at UHF frequencies, hexaferrites are comparatively unique in offering control over  $\mu_r$  and  $\epsilon_r$  at frequencies not coincident with extremely lossy ferromagnetic resonances associated with common spinel and Ni-Zn ferrites [6]. Observation of the recent literature indicates that while

$\mu_r$  and  $\varepsilon_r$  can be controlled, minimum loss tangent may not coincide with the desired  $\mu_r$  and  $\varepsilon_r$  values at a target frequency [7, 13]. Thus, the bandwidth advantage conferred by impedance matching the substrate to the channel may be nullified by high loss tangent, resulting in low efficiency.

## 2.2 Review of hexaferrite antennas

Various miniaturised antennas have been reported with hexaferrite elements, including wire-wound conductors on hexaferrite chips [8, 9] and patches with substrates that were solid tiles [10, 11], flexible [3] or a lattice of hexaferrite bars [12]. While all of these works observed miniaturisation, varying approaches to performance analysis especially with regard to the treatment of loss tangent and efficiency lead to differing conclusions on the applicability of the antenna to various communication problems.

Where high radiation efficiencies have been reported, these appear to be limited to designs which use hexaferrite chip loading elements such as [8, 9, 12], where the miniaturisation is less pronounced than that observed in conventional patch designs due to the lower filling factor. Conventional patch designs achieve greater miniaturisation [10, 11, 3] but the utility of these designs for common communication problems depends on whether loss tangent and efficiency has been given full consideration. The works of [10, 11] overlook loss tangent, wherein LTE MIMO is proposed as a possible application. Without an analysis of loss tangent, this view may be compromised by low radiation efficiency.

In contrast, works presenting detailed analysis of the loss tangents in hexaferrite patches such as [3] advance the view that hexaferrite patches are mostly applicable to short range communications such as RFID or health monitoring. The low gain of even relatively low-loss hexaferrites makes hexaferrite miniaturisation best suited to cases where miniaturisation is of paramount importance compared to concerns of efficiency.

## 3 Antenna design

### 3.1 Material characterisation

The hexaferrite was a composite of 75%  $\text{Co}_2\text{Z}$ -phase to 25%  $\text{Co}_2\text{Y}$ -phase ferrite [13], chosen for its near-balanced  $\varepsilon_r$  and  $\mu_r$  at UHF frequencies. Additionally, that work gave sufficient detail of the fabrication procedure to allow an external supplier to attempt to reproduce the material characteristics (Trans-Tech Inc., USA). The impedance characteristics of the hexaferrite material were measured using a Keysight E4991B impedance analyser over the frequency range 1–1000 MHz (Figure 1), along with those of FR-4 and Rogers RT5880 (plots omitted for brevity). The wave impedance  $Z$  (Eqn. 1) of each sample is given in Figure 2.

While the balanced-impedance criterion  $Z = Z_0$  was only satisfied in the hexaferrite sample at a single frequency of 944 MHz, it can be seen by inspection that the  $\text{Co}_2\text{Z}$  hexaferrite was better

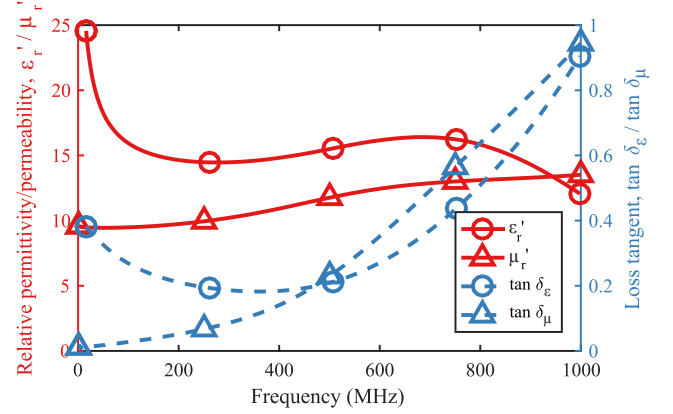


Fig. 1: Relative real permittivity, real permeability and loss tangent characteristics of hexaferrite sample.

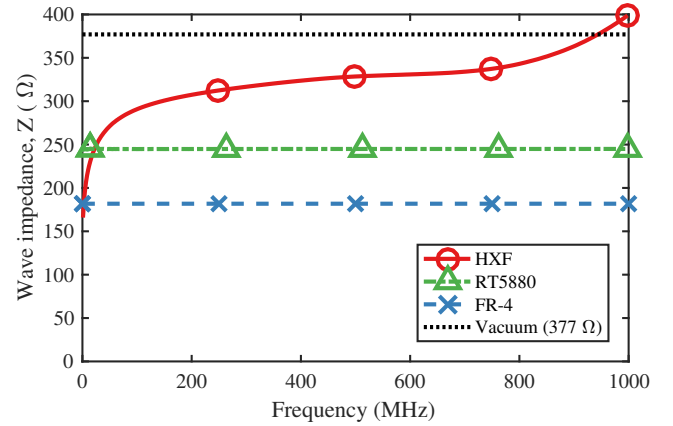


Fig. 2: Substrate wave impedance  $Z$  (Eqn. 1).

matched to the medium than the dielectric substrate samples. However, the loss tangents in the hexaferrite material were considerably higher than those measured for the dielectric materials, and also higher than those reported for the reference hexaferrite (Z75) as compared in Table 1. Ceramic UHF properties are recognised to be dependent on the material processing history [13], hence some variation from the reference characteristics was expected.

Material	Frequency (MHz)	$\varepsilon_r$	$\mu_r$	$\tan \delta_\varepsilon$	$\tan \delta_\mu$
HXF	329	14.5	10.4	0.18	0.10
HXF	450	15.1	11.3	0.19	0.18
HXF	650	16.3	12.7	0.32	0.42
“Z75” [13]	650	13.5	12.3	0.04	0.25
FR-4	1–1000	4.4	-	0.015	-
RT5880	1–1000	2.3	-	0.0003	-

Table 1: Selected substrate UHF characteristics.

### 3.2 Antenna layout selection

A set of hexaferrite patch antennas were designed and simulated with the layouts given in Figure 3. The patch widths (50.0, 35.0 mm) were selected to target two frequencies: the lowest frequency available (subsequently measured to be 329 MHz), and 433 MHz (ISM band). The patch lengths (33.0, 15.0 mm) and feed track positions were selected to provide impedance matching to a 50  $\Omega$  coaxial line. The hexaferrite tiles were limited to maximum dimensions of 50 mm  $\times$  50 mm  $\times$  2 mm by the manufacturing process. The dimensions were maintained for antennas fabricated on FR-4 and RT5880 substrate to permit a study of antenna miniaturisation based predominantly on the change in substrate, except for varying the feed position to obtain a suitable feed match.

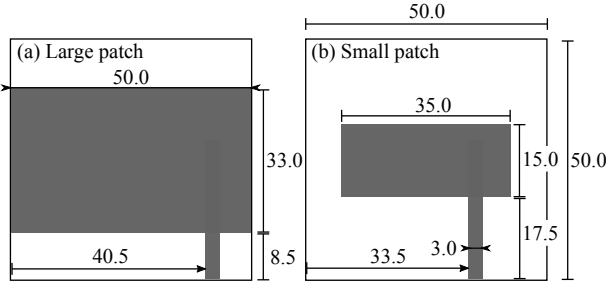


Fig. 3: Hexaferrite patch antenna layout. Dimensions in mm.

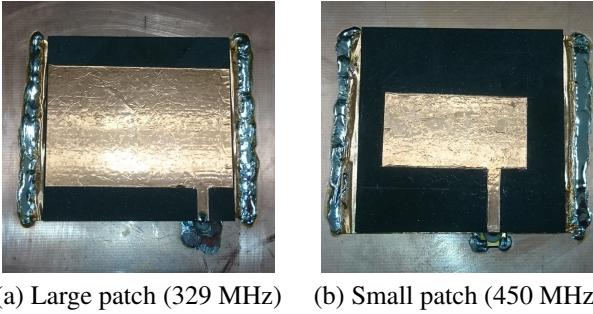


Fig. 4: Fabricated hexaferrite patch antennas.

## 4 Antenna Measurements

### 4.1 Input response

The simulated and measured input responses ( $S_{11}$ ) are shown in Figure 5, demonstrating the frequency reduction caused by the increased refractive index of the hexaferrite material. The frequency reduction factor is given relative to the measured frequency of the RT5880 antenna in each case by  $\frac{f(\text{RT5880})}{f(\text{meas})}$  in Table 2. The electrical smallness factor  $ka = 2\pi a/\lambda_0$  is calculated, where  $a = 35.4$  mm is the radius of the smallest sphere inscribing the antenna and feed track within its limits. Antennas with  $ka$  factors smaller than 0.5 may be classed as electrically small and are susceptible to exhibiting low radiation resistance  $r_{\text{rad}}$ , which may subsequently lead to low radiation efficiency even for modest substrate loss factors [4].

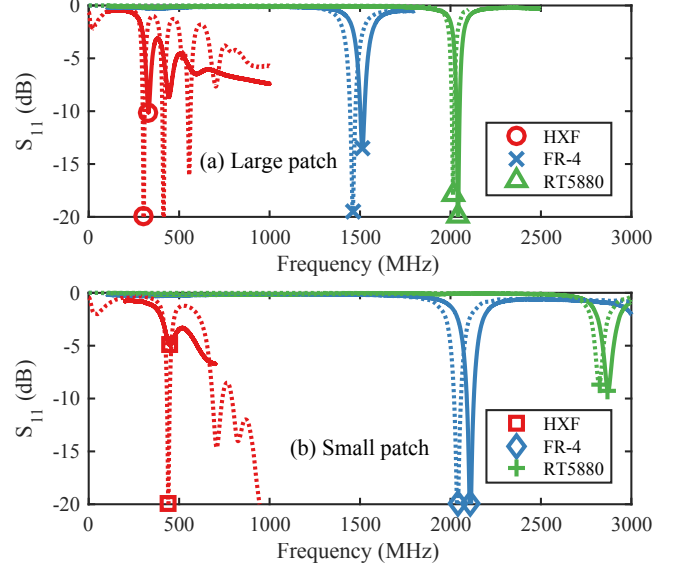


Fig. 5: Input response  $S_{11}$  of patch antennas. Solid lines denote measured results, dashed lines denote simulated results.

Antenna	Freq. (MHz)	Frequency reduction factor	$ka$
HXF large	329	6.2	0.24
FR-4 large	1514	1.3	1.12
RT5880 large	2042	(1)	1.51
HXF small	450	6.4	0.33
FR-4 large	2110	1.4	1.56
RT5880 large	2872	(1)	2.14

Table 2: Frequency reduction and electrical smallness  $ka$ .

### 4.2 Radiation patterns

The 3D measurement system is shown in Figure 6. The antenna under test (AUT) was aligned in the  $xy$ -plane, centred on a circular ground plane measuring 400 mm in diameter.

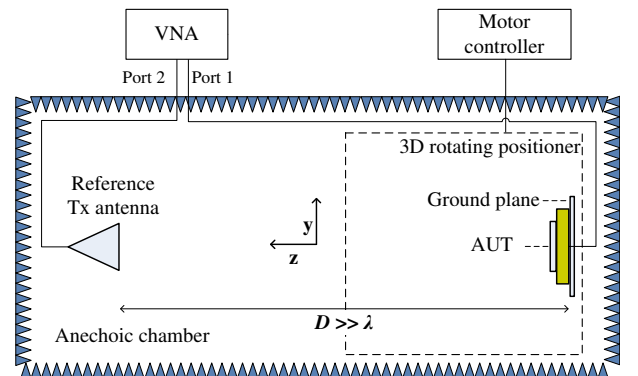
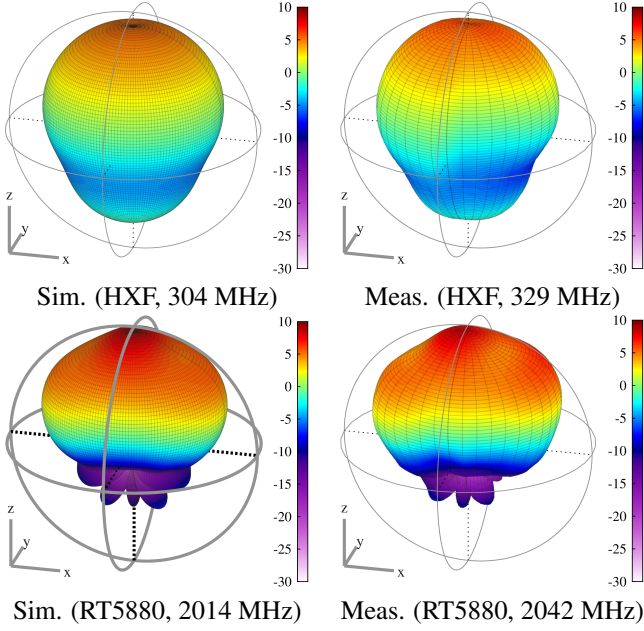


Fig. 6: Radiation pattern measurement setup in anechoic chamber.

3D radiation patterns were recorded for two orthogonal polarisations  $E_\theta$  and  $E_\phi$ , with positioner resolutions of  $\Delta\theta = 1^\circ$

and  $\Delta\phi = 10^\circ$ . For brevity, only total power  $E_{\text{total}}$  patterns can be given here. The power patterns measured at the resonant frequencies of the hexaferrite and RT5880 antennas are compared to the simulated patterns in Figures 7 and 8. The patterns were consistent with the  $TM_{10}$  mode, with the pattern similarity across the frequency range indicating that the radiating mode did not change. The increase in directivity with frequency was an artefact of the increasing electrical size of the fixed ground plane with respect to the decreasing operating wavelength, reducing diffraction into the  $-z$  hemisphere.



**Fig. 7:**  $E_{\text{total}}$  directivity patterns for large patch antenna.

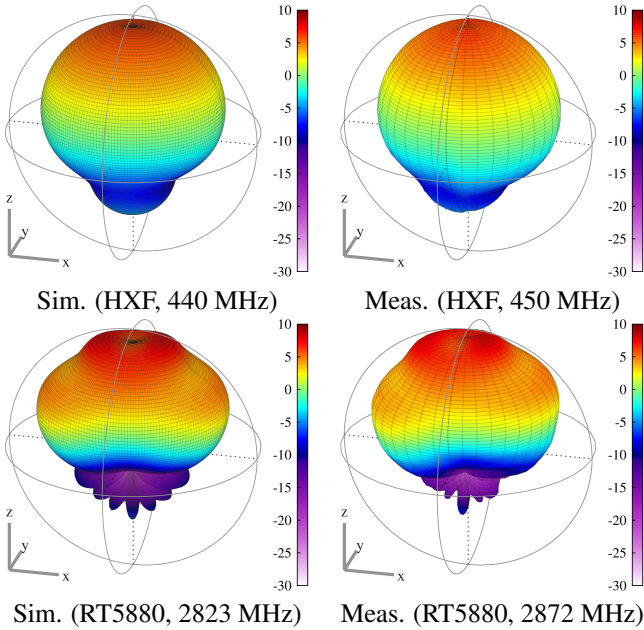


**Fig. 8:**  $E_{\text{total}}$  directivity patterns for small patch antenna.

### 4.3 Radiation efficiency

The radiation efficiency was calculated via a pattern integration method [14]. The total efficiency  $\eta = \eta_m \eta_\Omega$  is given by rearrangement of gain  $G = (\eta_m \eta_\Omega) D$ , with directivity  $D$  and matching efficiency  $\eta_m$ . Radiation efficiency  $\eta_\Omega$  consists of losses in the conductor, the substrate and the radiation resistance  $r_{\text{rad}}$ :

$$\eta_{\Omega, \text{AUT}} = \frac{r_{\text{rad}}}{r_{\text{rad}} + r_{\text{loss}}} \quad (2)$$

The pattern-integrated received power of the AUT was measured relative to that of a wire  $\lambda/4$  monopole constructed for each frequency to determine total efficiency  $\eta_m \eta_\Omega$ . The ratio of overall efficiencies  $\eta_{\text{AUT}}/\eta_{\text{ref}}$  permits efficiency calculation since the quarter-wave metallic monopole is recognised to be highly efficient [14], thus for comparison purposes it can be assigned a radiation efficiency value of  $\eta_{\Omega, \text{ref}} = 1$ . Scaling the measured overall efficiency ratio by the matching efficiencies yields a measure of the radiation efficiency for the AUT at each frequency:

$$\frac{\eta_{\Omega, \text{AUT}}}{(\eta_{\Omega, \text{ref}} = 1)} = \frac{\eta_{\text{AUT}}}{\eta_{\text{ref}}} \times \frac{\eta_{m, \text{ref}}}{\eta_{m, \text{AUT}}} \quad (3)$$

The radiation efficiencies given by Eqn. 3 are given in Figure 9 for each of the antennas.

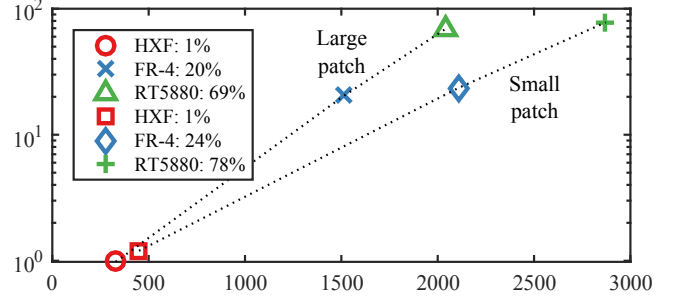


**Fig. 9:** Radiation efficiency relative to reference  $\lambda/4$  wire monopole of low loss.

The RT5880 substrates delivered greater radiation efficiency than the FR-4 substrate, which was in turn much more efficient than the hexaferrite substrate. This can be understood as a combined effect of increased loss tangent of hexaferrite and FR-4 than that of RT5880 and falling  $r_{\text{rad}}$  as the electrical size of the antenna is reduced with respect to the free space wavelength (documented by the  $ka$  factor in Table 2).

Electrically small antennas with  $ka < 0.5$  are recognised to be susceptible to low radiation resistance, reducing efficiency even for fixed values of substrate loss (Eqn. 2) [4]. While the hexaferrite antennas remained resonant in terms of substrate wavelength, they nevertheless had small physical apertures. The authors therefore contend that while the loss tangents of the hexaferrite materials in development might be considered



low with respect to other ferrites in the UHF band by material scientists [13], the loss tangents need to be reduced much more aggressively to cope with the reduced  $r_{\text{rad}}$  coincident with the enhanced miniaturisation offered by hexaferrite substrates.

## 5 Conclusions

A magneto-dielectric hexaferrite substrate was characterised across the frequency range 1–1000 MHz. At the tested antenna frequencies of 329 MHz and 450 MHz it was found to have a refractive index of  $n = \sqrt{\mu_r \times \epsilon_r} = 12.3/13.0$  and loss tangents of approximately  $\tan \delta_\epsilon = 0.18$  and  $\tan \delta_\mu = 0.10 - 0.18$ . The hexaferrite material exhibited a close wave impedance match to  $377 \Omega$  across the measured band. The high refractive index and reasonably high filling factor of the substrate compared to *e.g.* hexaferrite-chip loaded designs gave a frequency reduction factor greater than six relative to the same-sized antenna on Rogers RT5880 substrate.

The low measured efficiency of the hexaferrite antennas suggests that material loss tangent has a profound effect on the utility of hexaferrite materials, potentially precluding hexaferrite use for efficient miniaturisation of patch antennas for long range communication. On the balance of the challenges of efficiency versus miniaturisation, the authors are in agreement with the findings of [3] that hexaferrite patch antennas are best suited to miniaturisation-critical applications such as short range antennas for wearable or RFID applications, or compact receivers where the received signal strength is already low. Determination of target loss tangents for efficient performance with respect to rapidly reducing  $r_{\text{rad}}$  with increasing miniaturisation could represent an extension to the present work.

## Acknowledgements

The authors wish to thank the UK Engineering and Physical Sciences Research Council (EPSRC) Centre for Doctoral Training (CDT) in Communications (EP/I028153/1) for financial support. The authors also wish to thank Keysight Technologies for the loan of the E4991B Impedance Analyser used in this work.

## References

- [1] Ofcom, “OfW570: Guidance for manually configurable white space devices,” Ofcom, Tech. Rep., September 2016.
- [2] Federal Communications Commission, “Unlicensed Operation in the TV Broadcast Bands/Additional Spectrum for Unlicensed Devices Below 900 MHz and in the 3 GHz Band,” FCC (USA), Tech. Rep. FCC 12-36, Apr. 2012.
- [3] L. J. Martin, S. Ooi, and D. Staiculescu, “Effect of permittivity and permeability of a flexible magnetic composite material on the performance and miniaturization capability of planar antennas for RFID and wearable wireless applications,” *IEEE Transactions on Components and Packaging Technologies*, vol. 32, no. 4, pp. 849–858, Dec 2009.
- [4] J. D. Kraus and R. J. Marhefka, *Antennas for all Applications*, 3rd ed. McGraw-Hill, 2002.
- [5] R. Hansen and M. Burke, “Antennas with magneto-dielectrics,” *Microwave and Optical Technology Letters*, vol. 26, no. 2, pp. 75–78, Jul 2000.
- [6] S. Fujii, K. Wakamatsu, H. Satoh *et al.*, “Wide bandwidth CuO-modified  $\text{Ba}_2\text{Co}_2\text{Fe}_{12}\text{O}_{22}$  ferrite antenna,” *IEEE Antennas and Wireless Propagation Letters*, vol. 15, pp. 1171–1174, 2016.
- [7] Z. Zheng, Q. Feng, Q. Xiang *et al.*, “Low-loss NiZnCo ferrite processed at low sintering temperature with matching permeability and permittivity for miniaturization of VHF-UHF antennas,” *Journal of Applied Physics*, vol. 121, no. 6, p. 063901, 2017.
- [8] S. Bae, Y. K. Hong, J. J. Lee *et al.*, “Miniaturized broadband ferrite T-DMB antenna for mobile-phone applications,” *IEEE Transactions on Magnetics*, vol. 46, no. 6, pp. 2361–2364, June 2010.
- [9] W. Lee, Y. K. Hong, J. Lee *et al.*, “Dual-polarized hexaferrite antenna for unmanned aerial vehicle (UAV) applications,” *IEEE Antennas and Wireless Propagation Letters*, vol. 12, pp. 765–768, 2013.
- [10] Q. Zhang, Z. Chen, Y. Gao *et al.*, “Miniaturized antenna array with Co2Z hexaferrite substrate for massive MIMO,” in *2014 IEEE Antennas and Propagation Society International Symposium (APSURSI)*, July 2014, pp. 1803–1804.
- [11] Z. Chen, J. Yu, X. Chen *et al.*, “UHF tunable compact antennas on Co2Z hexaferrite substrate with 2.5/1 tunable frequency range,” in *2015 IEEE International Symposium on Antennas and Propagation USNC/URSI National Radio Science Meeting*, July 2015, pp. 2287–2288.
- [12] W. Lee, Y. K. Hong, J. Park *et al.*, “Low-profile multi-band ferrite antenna for telematics applications,” *IEEE Transactions on Magnetics*, vol. 52, no. 7, pp. 1–4, July 2016.
- [13] Z. Su, Q. Li, X. Wang *et al.*, “Tunable permittivity and permeability of low loss Z + Y-type ferrite composites for ultra-high frequency applications,” *Journal of Applied Physics*, vol. 117, no. 17, p. 17E506, 2015.
- [14] D. L. Paul, H. Giddens, M. G. Paterson *et al.*, “Impact of body and clothing on a wearable textile dual band antenna at digital television and wireless communications bands,” *IEEE Transactions on Antennas and Propagation*, vol. 61, no. 4, pp. 2188–2194, April 2013.